Tumor Necrosis Factor–dependent Segmental Control of MIG Expression by High Endothelial Venules in Inflamed Lymph Nodes Regulates Monocyte Recruitment

Mary J. Janatpour,[1, 3] Susan Hudak,[1, 2] Manjiri Sathe,[1]
Jonathon D. Sedgwick,[1] and Leslie M. McEvoy[1, 2]

[1]*DNAX Research Institute, and* [2]*Corgentech, Inc., Palo Alto, CA 94304*
[3]*Chiron Corporation, Emeryville, CA 94608*

Abstract

Monocytes recruited from the blood are key contributors to the nature of an immune response. While monocyte recruitment in a subset of immunopathologies has been well studied and largely attributed to the chemokine monocyte chemoattractant protein (MCP)-1, mechanisms mediating such recruitment to other sites of inflammation remain elusive. Here, we showed that localized inflammation resulted in an increased binding of monocytes to perifollicular high endothelial venules (HEVs) of lymph nodes draining a local inflammatory site. Quantitative PCR analyses revealed the upregulation of many chemokines in the inflamed lymph node, including MCP-1 and MIG. HEVs did not express detectable levels of MCP-1; however, a subset of HEVs in inflamed lymph nodes in wild-type (but not tumor necrosis factor [TNF] null mice) expressed MIG and this subset of HEVs preferentially supported monocyte binding. Expression of CXCR3, the receptor for MIG, was detected on a small subset of peripheral blood monocytes and on a significant percentage of recruited monocytes. Most importantly, in both ex vivo and in vivo assays, neutralizing anti-MIG antibodies blocked monocyte binding to inflamed lymph node HEVs. Together, these results suggest that the lymph node microenvironment can dictate the nature of molecules expressed on HEV subsets in a TNF-dependent fashion and that inflammation-induced MIG expression by HEVs can mediate monocyte recruitment.

Key words: HEV • cell adhesion • microenvironment • homing • lymph node

Introduction

One of the first cell types to arrive at a site of inflammation is the blood monocyte. It has long been known that monocytes can differentiate into tissue macrophages, which in turn have phagocytic and antigen presentation capabilities. It is also known that monocytes can differentiate into dendritic cells (1, 2). Monocytes, themselves, and the cells they differentiate into produce a host of cytokines and chemokines and thus, in large part, dictate the cell types that are subsequently recruited to an inflammatory site. Thus, both by virtue of the cytokines they produce and by virtue of the cell types they differentiate into upon entering the tissue, monocytes recruited from the blood are key orchestrators of the nature of an immune response. While monocytes are critical to mounting an effective immune response, their presence in chronic inflammatory sites can be pathogenic. For example, monocyte recruitment is an initiating event in the advent of atherosclerotic lesions (for reviews, see references 3–5).

Chemokines are a class of cytokines with chemoattractant properties, as well as other functions. Several chemokines are capable of chemoattracting monocytes in vitro and, of these, monocyte chemoattractant protein (MCP)*-1 is among the most potent (6). Furthermore, MCP-1 and its receptor, CCR2, are found in atherosclerotic lesions (7, 8). Deleting genes for either MCP-1 or CCR2 attenuates the incidence of lesions in established models of atherosclerosis (9, 10) and appears to do so by blocking the recruitment of monocytes. More recently, MCP-1 and CCR2 have also

Address correspondence to Leslie M. McEvoy, 1651 Page Mill Rd., Palo Alto, CA 94304. Phone: 650-624-9600; Fax: 650-624-7540; E-mail: mcevoy@corgentech.com

**Abbreviations used in this paper:* EAE, experimental autoimmune encephalomyelitis; HEV, high endothelial venule; MCP, monocyte chemoattractant protein; PNAd, peripheral node addressin.

been implicated in the development of inflammatory lesions of experimental autoimmune encephalomyelitis ([EAE] references 11–13). Although monocyte recruitment in atherosclerosis and EAE has been well studied and largely attributed to the CC chemokine MCP-1, mechanisms mediating such recruitment to many other sites of inflammation remain elusive.

Leukocyte recruitment to and through the lymph node is critical to immune surveillance and to mounting an effective immune response. Leukocytes enter the lymph node via two routes: the afferent lymphatics (from the tissue) or the specialized endothelium, the high endothelial venules ([HEVs] from the blood). Leukocyte recruitment to the HEVs has been well studied (14, 15). The required molecular mechanisms, both adhesion molecules and chemokines and their receptors, orchestrating recruitment of naive T cells to lymph nodes have been largely defined (16–18). As has been shown previously, upon acute inflammation in the footpad, there is a selective increase in recruitment of monocytes to HEVs in the draining lymph node (19). The mechanisms mediating monocyte-selective recruitment in this setting are unknown. Here we examined the potential role of chemokines in mediating monocyte-selective increase in recruitment to HEVs in inflamed lymph nodes. Since TNF has been shown to be upstream of chemokine expression (20–22), the chemokine expression patterns and monocyte binding capability of inflamed lymph nodes from TNF null mice were also examined.

We show that whereas MCP-1 may be critical in monocyte recruitment in other systems, we were unable to demonstrate expression of this molecule on HEVs in normal or inflamed lymph nodes. Thus, MCP-1 expression cannot account for the recruitment observed, at least at the level of adhesion to the HEVs. Interestingly, HEVs display the CXC chemokine MIG in response to an inflammatory stimulus and this subset of HEVs has an enriched capacity to bind monocytes. In TNF null mice, the increase in the number of HEVs expressing MIG is not observed upon induction of inflammation, nor is there an increase in monocyte binding to HEVs, as seen in wild-type mice. Furthermore, function-perturbing antibodies to MIG block monocyte binding in both in vivo and ex vivo assay systems. Together, these results suggest that the lymph node microenvironment can dictate the nature of molecules expressed on HEV subsets in a TNF-dependent fashion and that MIG can mediate monocyte binding in an inflammatory response.

Materials and Methods

Footpad Injection and Isolation of Lymph Nodes. C57BL/6 mice (2–3 mo old) were obtained from The Jackson Laboratory; age and sex-matched $TNF^{-/-}$ mice (on a C57BL/6 background; reference 23) were bred in house. At day 0, mice (10–12 per group) were briefly anesthetized with isoflurane and 40 μl of complete Freund's adjuvant (5881; Sigma-Aldrich) was injected subcutaneously into the footpad of the forepaw through a 27-gauge needle. At day 3 (~72 h after injection), mice were killed and brachial lymph nodes were harvested. Brachial lymph node–draining footpads that were not inflamed were also harvested. All animal work was approved by an internal review board and met NIH Institute Animal Care and Use Committee standards. Lymph nodes were either snap-frozen for subsequent RNA isolation or embedded in O.C.T. Compound (4583; Tissue-Tek) for sectioning.

Real-Time Quantitative PCR (TaqMan™). Total RNA was extracted using RNA Stat 60 according to the manufacturer's instructions (CS110; Tel-Test). Total RNA was treated with DNase I (776-785; Roche Laboratories) to eliminate possible genomic DNA contamination. Total RNA was then reverse transcribed with oligo(dT)14–18 (18418; Life Technologies), random hexamers (C1181; Promega), dNTPs (27-2035; Amersham Pharmacia Biotech), and Superscript II (18064-014; Life Technologies), according to the manufacturer's instructions. 50 ng of cDNA was amplified using 12.5 μl of TaqMan™ universal master mix (PerkinElmer), 0.2 μM of gene-specific TaqMan™ probe, and 0.9 μM of gene-specific forward and reverse primers in a final volume of 25 μl. Primers and probes specific to each chemokine tested (see Fig. 1) were obtained from PerkinElmer. Ubiquitin mRNA levels were used to normalize between samples. Gene-specific PCR products were measured at each cycle, through 40 cycles, by means of a GeneAmp 5700 Sequence Detection System (PerkinElmer). mRNA levels were quantitated by comparing experimental levels to standard curves generated using serial dilutions of plasmids containing the chemokine gene being evaluated.

Immunohistochemistry. Primary antibodies that recognize the following antigens were used at the listed concentrations: B220 (10 μg/ml 01129A; BD PharMingen), peripheral node addressin ([PNAd] BD PharMingen) (15 μg/ml 09961D), CD11b (10 μg/ml M030055; BD PharMingen), 6CKine (CCL21; R&D Systems) (20 μg/ml BAF457), IP10 (30 μg/ml CXCL10; made in house), MCP-1 (CCL2; R&D Systems) (30 μg/ml BAF479), and MIG (CXCL9; R&D Systems) (20 μg/ml AF-492-NA and BAF492). 10-μm frozen sections were fixed in 2% paraformaldehyde for 10 min, blocked in PBS/2% BSA, and then incubated with primary antibodies for 1 h at room temperature. With the exception of the antibodies against B220 and CD11b, which were fluorescently conjugated, secondary antibodies were used at a 1:100 dilution for 30 min at room temperature. After appropriate secondary blocking, sections were then stained with a tertiary antibody. Antibodies to MCP-1 and IP10 were incubated with sections before fixation. In some cases, anti-MIG antibodies were injected in vivo and detected ex vivo using a FITC-conjugated secondary antibody. Stained sections were visualized under a fluorescent confocal microscope (Leica TCS SP).

In Vivo "Snapshot" Assay. 5-μm sections of lymph nodes were fixed in acetone at −20°C for 5 min, blocked in PBS/2% BSA, and subjected to double-indirect immunohistochemistry for PNAd and CD11b as described previously. Sections were visualized under a fluorescent microscope. All $PNAd^+$ vessels from 10 lymph nodes were counted and scored for the presence of at least one CD11b-bright cell. Percentage of HEVs with bound monocyte was calculated as (number of $PNAd^+$ vessels with associated CD11b-bright cell/total number of $PNAd^+$ vessels ×100).

In Vivo Blocking Studies. Inflammation was induced in footpads of forepaws, as described previously. 20 h before killing, 1 mg of antibody (either anti-MIG; R&D Systems, lot AGS01) or control (AB-108-C; R&D Systems) was injected intraperitoneally per mouse. At day 3 after induction of inflammation, mice were killed and brachial lymph nodes harvested and embedded for sectioning as described previously. Sections were either

stained with a FITC-conjugated secondary (anti–goat) antibody to localize injected primary antibody or subjected to the in vivo snapshot assay.

Ex Vivo HEV Binding Assay. A modification of the Stamper-Woodruff assay (24) was performed as follows. T cells were isolated from peripheral lymph nodes of Balb/c mice and WEHI 78/24 cells were subcultured to be in plateau phase at the time of the experiment. T cells and WEHI 78/24 cells were mixed in a 1:1 ratio (final concentration of 10^7cells per milliliter) in binding buffer (DMEM supplemented with 20 mM Hepes and 1% BSA, pH 6.9). 100 μl of the cell suspension was placed on each of four 10-μm frozen sections of lymph nodes (per condition) that had been circled using a hydrophobic slide marker (2 cm diameter). Slides were immediately placed on a rotating platform (70 rpm) at 4°C for 30 min. Slides were then fixed in ice cold PBS/2% glutaraldehyde. Preliminary experiments had shown that T cells bind uninflamed and inflamed HEVs equivalently (data not shown); therefore, T cells were used as an internal standard. WEHI 78/24 and T cells (distinguished by an extreme size difference) bound to the lymph node HEVs were counted under a phase microscope. 100 HEVs were counted, for each condition, over several lymph nodes and across four sections. Data is presented as WEHI 78/24 binding relative to the internal standard T cells. Data is normalized such that the WEHI 78/24:T cell ratio for uninflamed lymph node HEVs is set at 1 for all experiments. For antibody blocking experiments, sections were incubated at 4°C with blocking antibody (50 μg/ml) or control for 10 min before the addition of cells. Antibody remained present for the duration of the experiment.

FACS® Analysis. Balb/c mice (Taconic) were given a single intraperitoneal injection of 3 ml thyoglycollate (T-9032; Sigma-Aldrich). 2 d later, peritoneal cells were harvested using peritoneal lavage with 10 ml HBSS (BW04-315Q; Biowhittaker). The cells were counted, washed, and resuspended to 10^6 cells per milliliter in staining buffer: HBSS containing 2% FBS (BW14-501F; Biowhittaker) and 10 mM Hepes (17-737E; Biowhittaker). To block nonspecific staining, cells were incubated with 50 μg/ml rat IgG (I8015; Sigma-Aldrich) and Fc block (BD PharMingen) for 30 min at 4°C. Cells were subsequently incubated for 30 min at 4°C with either a biotin-conjugated rat anti–mouse CXCR3 mAb (LM22.23.17; DNAX) or a biotin-conjugated isotype control rat IgG2b (11182C; BD PharMingen) in staining buffer containing 50 μg/ml nonspecific rat IgG (to block nonspecific binding of Ig). Cells were washed and stained for 30 min at 4°C with FITC-conjugated anti–mouse CD11b, PE anti–mouse F4/80, or APC anti–mouse GR1 (BD PharMingen) plus cychrome-streptavidin. Cells were washed a final time, resuspended in staining buffer, and analyzed on a FacsCalibur™ (Becton Dickinson). PBMCs were isolated from normal human donors, incubated with Fc block plus 50 mg/ml mouse IgG (Becton Dickinson) for 30 min at 4°C, and subsequently stained with FITC-conjugated anti-CXCR3 (R&D Systems) or FITC-conjugated mouse IgG1, an isotype matched negative control (R&D Systems), APC-conjugated anti-CD14 (BD PharMingen), PE-conjugated anti-CD11c (BD PharMingen), and cychrome-conjugated anti-CD4 and anti-CD8 (BD PharMingen).

Results

The CXC Chemokine MIG (CXCL9) Is Upregulated at the mRNA Level in Inflamed Lymph Nodes. MCP-1/CCL2 appears to be critical for the recruitment of monocytes in atherosclerosis and EAE. To determine whether MCP-1 contributes to recruitment of monocytes to HEVs in inflamed lymph nodes we measured the MCP-1 (as well as other chemokines known to chemoattract monocytes) in normal lymph nodes and lymph nodes draining a local inflammation using real-time quantitative PCR (TaqMan™;

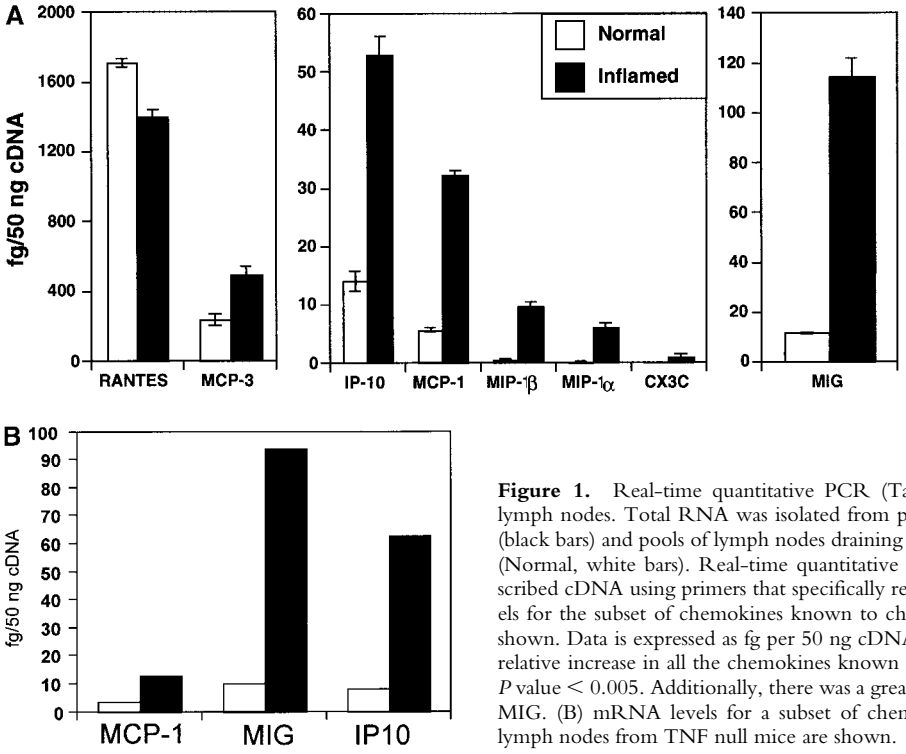

Figure 1. Real-time quantitative PCR (TaqMan™) analyses of chemokine expression in lymph nodes. Total RNA was isolated from pools of lymph nodes draining inflamed footpads (black bars) and pools of lymph nodes draining the contralateral footpads that were not inflamed (Normal, white bars). Real-time quantitative PCR was performed on 50 ng of reverse-transcribed cDNA using primers that specifically recognize a panel of chemokines. (A) mRNA levels for the subset of chemokines known to chemoattract monocytes in vitro and for MIG are shown. Data is expressed as fg per 50 ng cDNA. With the exception of RANTES, there was a relative increase in all the chemokines known to chemoattract monocytes, upon inflammation. P value < 0.005. Additionally, there was a greater than ninefold increase in the mRNA levels of MIG. (B) mRNA levels for a subset of chemokines in normal (not inflamed) and inflamed lymph nodes from TNF null mice are shown.

Fig. 1). Total RNA was isolated from pools of lymph nodes draining inflamed footpads and pools of lymph nodes draining the contralateral footpads that were not inflamed. Real-time quantitative PCR was performed on 50 ng of reverse-transcribed cDNA using primers that specifically recognize a panel of chemokines. mRNA levels for the subset of chemokines known to chemoattract monocytes in vitro and for MIG are shown in Fig. 1 A. With the exception of regulated on activation, normal T cell expressed and secreted (RANTES; CCL5), there was a relative increase in all the chemokines known to chemoattract monocytes (including MCP-1), upon inflammation in wild-type mice. Additionally, there was a greater than ninefold increase in the mRNA levels of MIG (from 12 fg/50 ng cDNA to 115 fg/50 ng cDNA), a chemokine which has not previously been shown to chemoattract monocytes.

TNF has been shown to play a key role in expression of many chemokines (20, 21); therefore, the role of TNF in induction of MIG was examined in TNF null mice. Failure of TNF null mice to upregulate TNF upon inflammation was confirmed by real-time quantitative PCR (data not shown). Examination of chemokine expression in TNF null lymph nodes before and after inducing inflammation revealed that whereas basal expression of a subset of chemokines was decreased relative to wild-type mice, confirming published reports (21), chemokine expression in inflamed lymph nodes of TNF null mice was upregulated to levels similar to those of wild-type lymph nodes. Examples of this are shown in Fig. 1 B.

Upon Inflammation, Recruitment of Monocytes to Lymph Node HEVs Is Increased in Wild-Type Mice, but not in TNF Null Mice. We quantitated the increased monocyte recruitment across lymph node HEVs upon inflammation using an in vivo "snapshot" assay (Fig. 2). 3 d after inducing inflammation, lymph nodes draining either inflamed footpads or footpads that were not inflamed were embedded in O.C.T. and sectioned. Double-indirect immunohistochemistry was performed to identify HEVs ($PNAd^+$, red; Fig. 2 inset) and monocytes (CD11b-bright, green). These CD11b-bright cells are positive for CD68 and negative for CD3, CD19, and NK1.1 (data not shown). HEVs were counted and scored for the presence or absence of bound monocytes at the time of sacrifice and percentage of total HEVs with one or more monocytes bound was calculated.

Induction of inflammation in the footpads of wild-type mice results in nearly a threefold increase in monocyte recruitment to lymph node HEVs (from 6 to 16%; Fig. 2). As TNF has been shown to be upstream of chemokine expression, we asked whether TNF null mice demonstrated an equivalent ability to recruit monocytes. Also shown in Fig. 2, TNF null mice have a reduced ability to recruit monocytes to HEVs upon inflammation, compared with wild-type mice.

MIG Protein Is Expressed on a Subset of HEVs in Wild-Type Lymph Nodes. While real-time quantitative PCR had indicated that a number of known monocyte chemoattractants were up-regulated upon inflammation in the lymph node at the mRNA level, the protein localization of

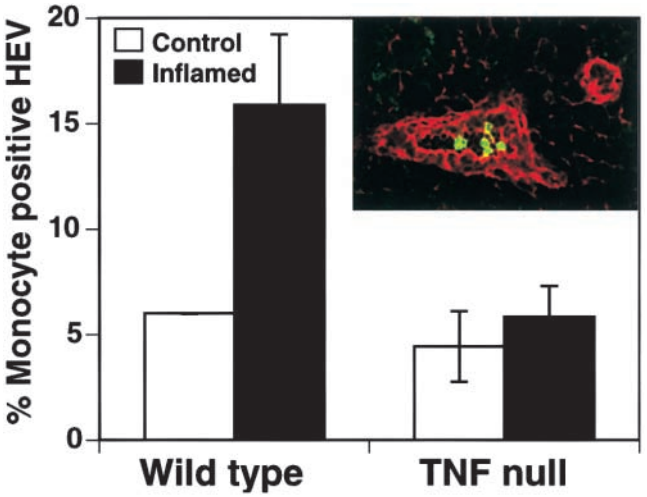

Figure 2. Recruitment of monocytes to lymph node HEVs is increased in wild-type mice, but not in TNF null mice, upon inflammation. 3 d after inducing inflammation, lymph nodes draining either inflamed footpads (black bars) or footpads that were not inflamed (white bars) were embedded in O.C.T., sectioned and subjected to the snapshot assay. Double-indirect immunohistochemistry was performed to identify all HEVs (red; see inset) and monocytes (green). The data is presented as percentage of total HEVs with at least one bound monocyte. Inducing inflammation in the footpads of wild-type mice results in nearly a threefold increase in monocyte recruitment to lymph node HEVs. TNF null mice have a reduced ability to recruit monocytes to HEVs upon inflammation, compared to wild-type mice. This experiment was repeated four times for wild-type mice and three times for TNF null mice. P value < 0.05.

these chemokines within the lymph node remained unclear. Based on the dominant role MCP-1 plays in monocyte recruitment in atherosclerosis, we expected that MCP-1 would be expressed prominently on HEVs. We also speculated that IP10 might be expressed on the HEVs, given that its mRNA induction was amongst the highest of the known monocyte chemoattractant chemokines (Fig. 1 A).

Serial sections of inflamed lymph nodes were subjected to double-indirect immunohistochemistry (Fig. 3 A). On all sections, an antibody against the B cell marker B220 was used to illuminate the B cell follicles for orientation. Serial sections were stained with antibodies against PNAd to identify HEVs, IP10, MCP-1 or an isotype control. While both MCP-1 and IP10 were highly expressed in macrophage-rich areas, to our surprise neither was displayed on HEVs (Fig. 3 A).

Because MIG was strongly induced upon inflammation at the mRNA level, we examined its protein expression as well (Fig. 3 B). Two staining methods were used. In the right panel, serial frozen-sections were stained with directly conjugated anti-6Ckine and anti-MIG antibodies and analyzed by confocal microscopy. The B cell follicle is outlined (based on B220 staining in a serial section). MIG was expressed on a subset of $6CKine^+$ HEVs close to the B cell follicle/T cell border. $6Ckine^+MIG^-$ HEVs were observed in the T cell zone and $6Ckine^+MIG^+$ HEVs were observed in the perifollicular area. Some HEVs (an example is indicated by the white arrow) show colocalization of 6Ckine and MIG (seen as yellow). The yellow arrow indi-

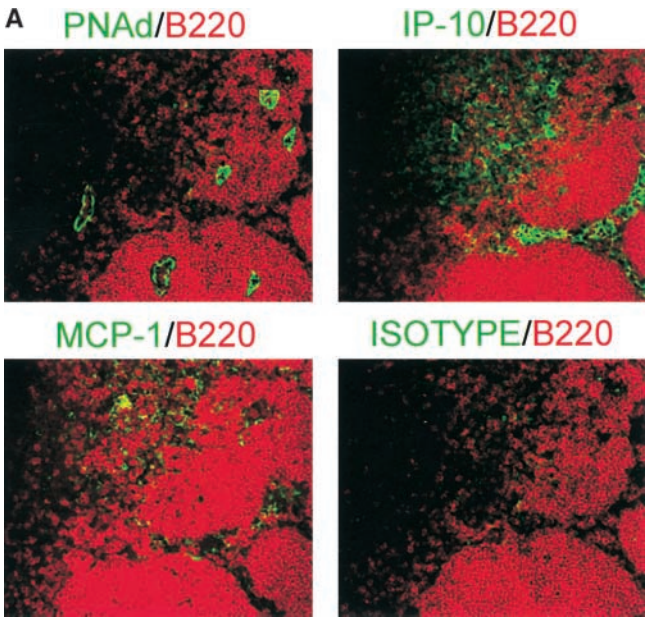

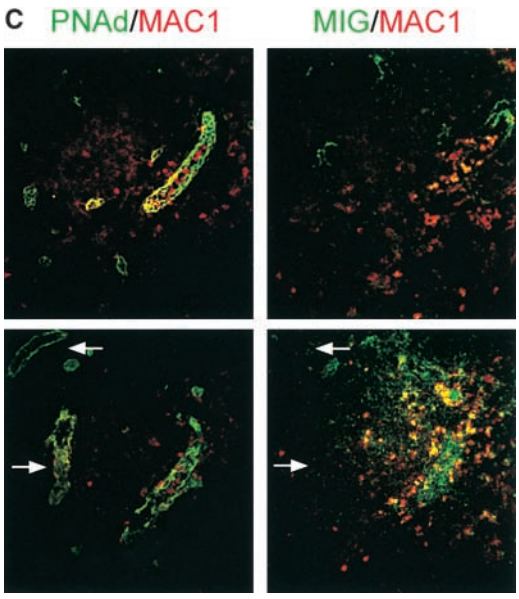

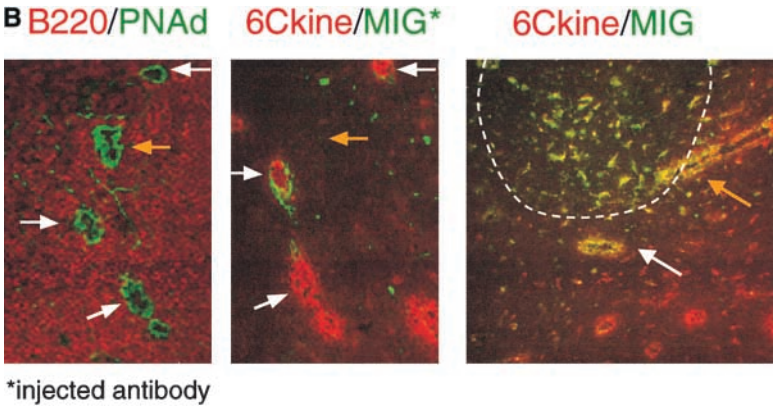

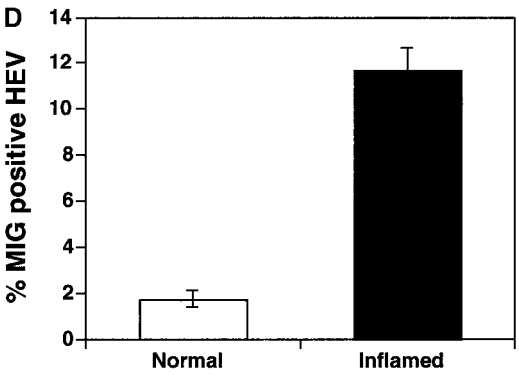

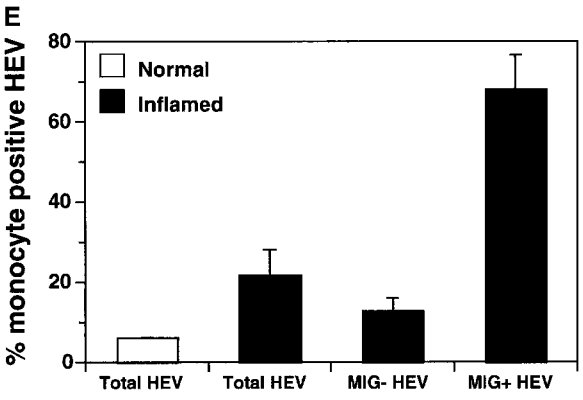

Figure 3. MIG expression on HEVs is correlated with increased monocyte-selective recruitment. (A) Serial sections of lymph nodes draining inflamed footpads were stained with antibodies against PNAd (top left panel, green) to identify HEVs, IP10 (top right panel, green), MCP-1 (bottom left panel, green), or an isotype control (bottom right panel, green). On all sections, an antibody against the B-cell marker B220 (red) identified the follicles and was used for orientation. MCP-1 and IP10 was not displayed on HEVs, but rather in macrophage-rich areas. (B) Serial sections (left and middle panels) were stained with either antibodies against PNAd (left panel, green) and B220 (left panel, red) or MIG (middle panel, green) and 6CKine (middle panel, red). MIG was expressed on a subset of 6CKine$^+$ HEVs. White arrows pair vessels between left and middle panels; yellow arrow indicates a vessel that is absent in the section represented in the middle panel. The right panel depicts vessels that were stained in vitro for 6CKine (red) and MIG (green). The outline depicts the B cell follicle border. Arrows depict vessels in which expression is completely colocalized (white) or partially colocalized (yellow). (C) Serial sections of lymph nodes draining inflamed footpads were stained for PNAd (left panels, green) and CD11b (red) or MIG (right panels, green) and CD11b (red). MIG$^+$ HEVs showed a higher association with monocytes than MIG$^-$ HEVs (arrows indicate MIG$^-$ vessels). (D) Serial sections were stained with antibodies against PNAd and MIG. The number of PNAd$^+$ and MIG$^+$ vessels was then counted across 10 lymph nodes. Data is presented as the percentage of total HEVs that were MIG$^+$. Lymph nodes that were not inflamed (white bar) had $<$2% MIG$^+$ HEVs. Upon inflammation (black bar), the number of MIG$^+$ HEVs increased to $\sim$12%. This experiment was repeated twice. (E) Immunohistochemistry was performed as shown in C. All PNAd$^+$ (total HEVs) and MIG$^+$ vessels were counted and scored for whether a monocyte was bound. Data is presented as percentage of HEV$^+$ for at least one bound monocyte. Upon inflammation (black bars) this increased from $\sim$6% in lymph nodes that were not inflamed (white bar) to $\sim$20%. The percentage of the subpopulation of total inflamed HEVs that were MIG$^+$ and had a bound monocyte was $>$60%; whereas, the percentage of the MIG$^-$ HEV subpopulation that had a bound monocyte was only 13%. This experiment was repeated twice.

cates an HEV when showed colocalization of MIG and 6Ckine staining in the region closer to the follicle and less MIG staining further away from the follicle. There are several HEVs that are 6Ckine$^+$ and MIG$^-$ as well. Thus, MIG is expressed on a subset of 6Ckine$^+$ vessels, predominantly in the perifollicular region of the lymph node. MIG was also expressed in macrophage-rich areas (data not shown). In a second set of experiments, unconjugated anti-MIG antibody was injected into mice at the same concentrations used for the blocking experiments and after killing (2 h after injection) the distribution of the injected antibody was illuminated using FITC-labeled secondary antibody and HEVs were identified by staining with anti-6Ckine antibody. Interestingly, as shown in the middle panel of Fig. 3 B, the injected MIG antibody has localized to the HEVs but appears to be basolateral to the 6Ckine staining.

The Percentage of HEVs that Express MIG Protein Is Increased upon Inflammation in Wild-Type Mice. On gross examination of sections from inflamed and uninflamed lymph nodes stained with an antibody against MIG, it was apparent that the number of HEVs that expressed MIG was increased upon inflammation. To quantitate this observation, serial sections were stained with antibodies to PNAd and to MIG and the percentage of MIG$^+$ HEVs was calculated. As shown in Fig. 3 D, there is a striking (sixfold) increase in the percentage of HEVs that express MIG in inflamed lymph nodes compared with resting lymph nodes. Interestingly, there was no induction of MIG$^+$ HEVs in TNF null mice; the percentage of MIG$^+$ HEVs in both normal and inflamed lymph nodes was similar to that of uninflamed wild-type mice.

The Subset of HEVs that Express MIG has an Enriched Capacity for Binding Monocytes. Many of the HEVs that are capable of supporting monocyte binding are found in the peri-B cell follicle region of the lymph node, the same region in which MIG$^+$ HEVs are observed. Therefore, we asked whether HEVs that express MIG have an enriched capacity to bind monocytes using the in vivo snapshot assay. Serial sections were stained for PNAd, MIG, and monocyte markers (Fig. 3 C) and all PNAd$^+$ and MIG$^+$ vessels were scored for their capacity to bind monocytes. Indeed, the MIG$^+$ subpopulation of HEVs has a dramatically increased capacity to bind monocytes compared with MIG$^-$ HEVs and total HEVs (Fig. 3 E).

A Function-perturbing Antibody to MIG Blocks Monocyte Binding to Inflamed HEVs In Vivo. The correlation of MIG expression and monocyte binding is compelling; however, in order to determine whether there is a functional significance to this, we asked whether a function-perturbing anti-MIG antibody was able to block monocyte recruitment. For these experiments, mice that had received an inflammatory regimen were treated intraperitoneally with either control or anti-MIG antibodies.

To confirm that the antibodies reached and bound the HEVs, sections were stained with a FITC-conjugated secondary antibody to localize the intraperitoneally injected

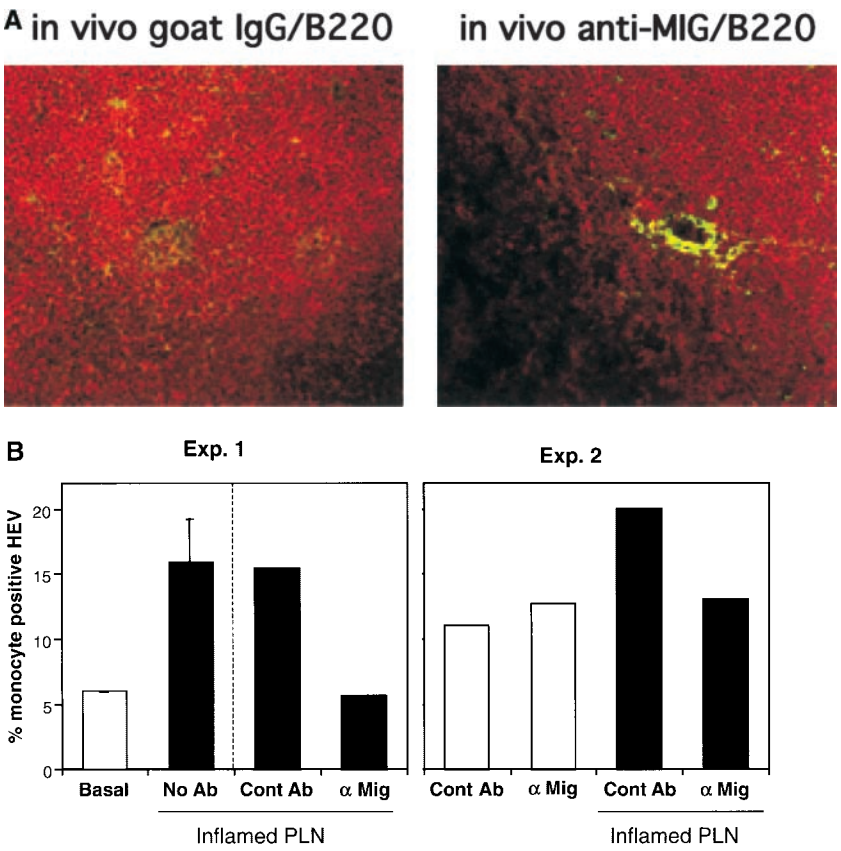

Figure 4. A function-perturbing antibody to MIG blocks monocyte binding to inflamed HEVs in vivo. To test whether MIG plays a role in monocyte recruitment to inflamed lymph nodes in vivo, inflammation was induced in both forepaws of 12 mice. The mice were divided into two groups, each receiving either a function-perturbing antibody to MIG or a control antibody intraperitoneally. In one experiment (Exp. 2), 12 mice that were not inflamed (white bars) also received the antibody treatment. Draining lymph nodes were isolated and sectioned. (A) To confirm that the antibodies reached and bound the HEVs, sections were stained with a FITC-conjugated secondary antibody to visualize the intraperitoneally injected antibody. Sections were costained with an antibody against B220. The neutralizing antibody to MIG localized to the HEV (right, green). (B) The in vivo snapshot assay was performed to determine the percentage of HEVs with a bound monocyte in the presence of either a MIG neutralizing antibody (αMIG) or the control (Cont Ab). 15–20% of inflamed HEVs had a bound monocyte in the presence of the control antibody, similar to what was observed in the absence of antibody (compare No Ab to Cont Ab, black bars). In the presence of a MIG neutralizing antibody this percentage was reduced to levels equivalent to uninflamed controls (white bars).

antibody. As shown in Fig. 4 A, the neutralizing antibody to MIG (but not the control antibody) localized to the HEVs (right panel, green) confirming display of MIG on the HEVs and presence of neutralizing antibody during the peak of monocyte recruitment.

The ability of HEVs to support monocyte binding in the presence of anti-MIG or control antibody was evaluated in two independent in vivo snapshot assays shown in Fig. 4 B. Due to limited amounts of neutralizing antibody, in one assay only mice receiving the inflammatory regimen were treated with control and anti-MIG antibody whereas both control and inflamed mice were included in the second experiment. In both cases, the percentage of HEVs able to support monocyte binding in the presence of control antibody was ~15–20%, in complete agreement with previous data. Strikingly, in both experiments, the presence of neutralizing anti-MIG antibody reduced monocyte binding to background levels. These results suggest that MIG plays a role in the recruitment of monocytes to inflamed HEVs.

Upon Inflammation, Binding of Monocytes to Lymph Node HEVs Ex Vivo Is Increased in Wild-Type Mice, but not in TNF Null Mice. In the in vivo assay, the anti-MIG blockade was in place for a significant period during the peak of monocyte recruitment to the inflamed lymph nodes opening up the possibility that MIG may be acting directly or indirectly. The Stamper-Woodruff frozen section ex vivo staining assay offers an excellent approach to study molecules presented on HEVs and their role in cell recruitment (24). We used this model to look at the ability of HEVs to bind a monocyte cell line, WEHI 78/24.

Local inflammation resulted in a selective increase in WEHI 78/24 binding capacity of HEVs analogous to the in vivo results. As shown in Fig. 5 A, lymph nodes from inflamed wild-type mice had a twofold increase in WEHI 78/24 binding to HEVs when compared with mice that were not inflamed. Furthermore, WEHI 78/24 binding to inflamed HEVs from TNF null mice was similar to that observed in uninflamed wild-type mice, also analogous to what was observed in vivo, suggesting that this ex vivo approach offers a reasonable assay system to model the in vivo mechanism.

A Function-perturbing Antibody to MIG Blocks Monocyte Binding to Inflamed HEV Ex Vivo. The twofold increase in WEHI 78/24 binding, although not profound, was consistent, allowing us to test whether MIG plays a direct role in monocyte adhesion at the surface of the HEVs. The Stamper-Woodruff assay was performed on both normal and inflamed lymph nodes (Fig. 5 B) in the presence of either a MIG neutralizing antibody, control, or no antibody. The control antibody had no effect on the induced WEHI 78/24 binding to inflamed HEVs; however, in the presence of a MIG-neutralizing antibody WEHI 78/24 binding was reduced to background binding levels. These results suggest that MIG may directly mediate monocyte adhesion to HEVs but do not eliminate the potential for additional mechanisms.

A Subset of Monocytes Expresses CXCR3. CXCR3 is the only known receptor for MIG. We asked whether a

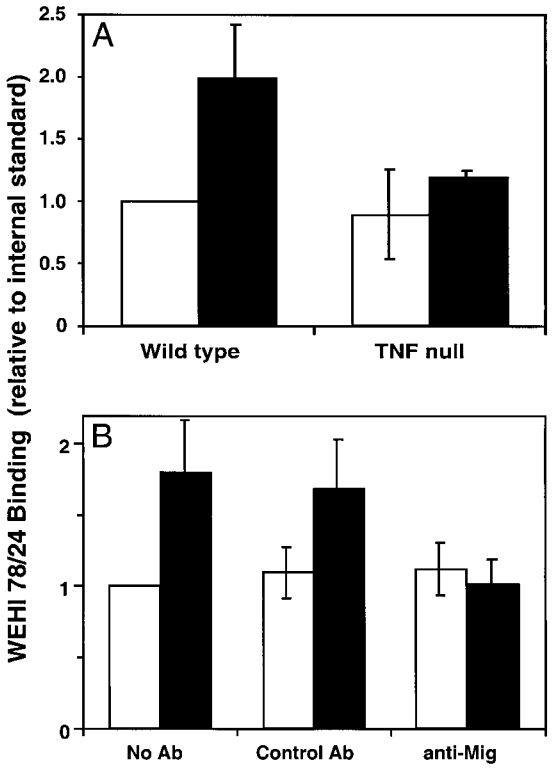

Figure 5. MIG may play a direct role in monocyte-selective recruitment in inflammation. (A) Frozen lymph node sections were incubated with cells under nonstatic, cold conditions, and the ability of the HEVs to bind WEHI 78/24 was quantitated. Data is expressed as WEHI binding relative to an internal standard. Lymph nodes from inflamed (black bars) wild-type mice had a twofold increase in WEHI 78/24 binding to HEVs when compared to mice that were not inflamed (white bar; P value $<$ 0.01). Furthermore, monocyte binding to inflamed HEVs from TNF null mice was similar to that observed in uninflamed wild-type mice, analogous to what was observed in vivo. This experiment was repeated three times. (B) The ex vivo assay described previously was performed on both inflamed lymph nodes (black bars) or lymph nodes that were not inflamed (white bars) in the presence of either a MIG neutralizing antibody (anti-MIG), a control (Control Ab), or no antibody at all (No Ab). In the presence of the control antibody, there was approximately a twofold increase in monocyte binding to inflamed HEVs compared to uninflamed HEVs (P value $<$ 0.05). This was similar to that observed in the absence of antibody. In the presence of a MIG-neutralizing antibody, however, the degree of monocyte binding to inflamed HEVs was reduced to background levels. This experiment was repeated three times.

$CXCR3^+$ population of monocytes could be found in circulating blood. It is extremely difficult to obtain circulating monocytes from the mouse; therefore, the CXCR3 expression of human blood monocytes was analyzed by flow cytometry. A small population of blood monocytes (defined as $CD11c^+CD14^+CD4^-CD8^-$ mononuclear cells) expressing CXCR3 was detected in two individual donors (1.91 and 1.70%, respectively; two isotype-matched negative controls gave 0.12% and this background has been subtracted). These results confirm those reported previously (25) showing that CXCR3 was expressed on 1 ± 1% of normal peripheral blood monocytes and 8 ± 4% of peripheral blood monocytes from patients with rheumatoid arthritis. An interesting population of "plasmacytoid mono-

cytes" that express CXCR3 (and L-selectin) has been described in inflamed lymph nodes in and around the HEVs (26). The relationship between these cells and the subpopulation of peripheral blood CXCR3$^+$ monocytes is not clear but could provide some insight on this specialized cell lineage.

Together these data prompted us to ask whether newly recruited monocytes express CXCR3. To obtain an enriched population of recruited monocytes, mice were injected with thyoglycollate intraperitoneally and the elicited cells were harvested by peritoneal lavage. Cells were stained for CXCR3, CD11b, F4/80. and GR1 and analyzed by FACS®. As shown in Fig. 6, a significant percentage of the newly recruited monocytes express CXCR3, as compared with the isotype control and GR1$^+$ neutrophils.

Discussion

Chemokines have emerged as an important class of molecules in directing selective recruitment of leukocyte subsets to tissue microenvironments and sites of inflammation. They, in conjunction with adhesion molecules, provide a highly regulated and selective mechanism for recruitment and microenvironmental localization of specific cell subsets to tissues, and immune and inflammatory sites. We observed previously that after induction of inflammation there is a striking monocyte-selective increase in binding to HEVs in inflamed lymph nodes (19) that could not be explained solely by adhesion molecules known to play a role in both monocyte and T cell recruitment. We used this striking model of monocyte-selective recruitment to test the hypothesis that monocyte chemoattractant chemokines (such a MCP-1) might provide an additional level of regulation in the specific recruitment of monocytes upon inflammation. Surprisingly, MCP-1, a potent monocyte chemoattractant shown to be key in recruitment of monocytes in EAE and models of atherosclerosis, was not displayed on the HEVs, but rather, was restricted to the macrophage population (Fig. 3 A) and it is therefore unlikely that MCP-1 can explain the monocyte-selective recruitment observed.

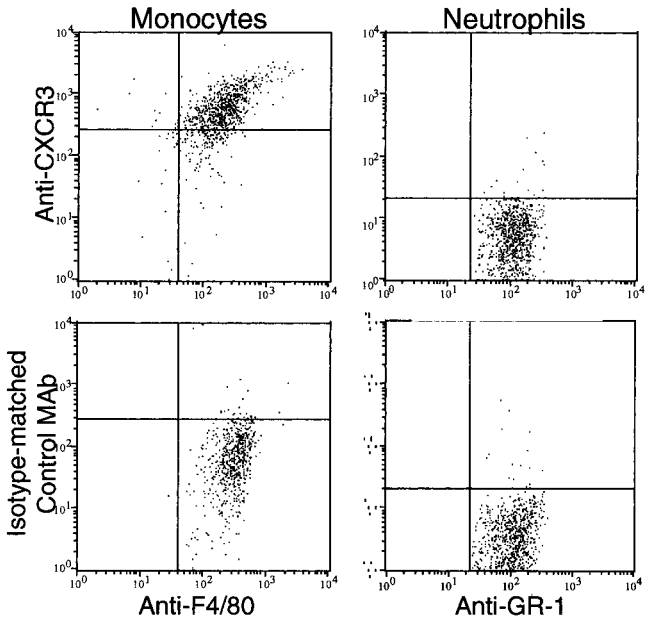

Figure 6. Newly recruited monocytes express CXCR3. Balb/C mice were given a single intraperitoneal injection of thyoglycollate. 2 d later, peritoneal cells were harvested and stained for CXCR3 or an isotype control (CyC), CD11b (FITC), F4/80 (PE), and GR1 (APC). Gates were set on newly recruited monocytes (CD11b$^+$) and neutrophils (GR1$^+$), after selection based on size and side-scatter. A significant percentage of monocytes recruited to the peritoneum expressed CXCR3 (compared to isotype control) whereas the neutrophil population did not.

Further immunohistochemical analysis revealed that a subset of HEVs surrounding the B cell follicles (a subcompartment of lymph nodes) displayed the chemokine MIG. Colocalization studies using confocal microscopy showed that 6Ckine and MIG are colocalized in many perifollicular HEVs while HEVs in the T cell zones express 6Ckine but very little MIG. Interestingly, when the distribution of anti-MIG antibody was assessed after intraveneous injection (followed by ex vivo staining for the presence of the anti-MIG antibody as well as 6Ckine) the anti-MIG antibody was localized basolateral to that of the 6Ckine staining. It is not clear if the altered staining pattern reflects a redistribution of the injected antibody and/or the antigen during the in vivo incubation period; however, it is interesting to speculate that antigen distribution over time could play a role in recruitment.

The subset of HEVs that support monocyte binding were also perifollicular prompting us to test whether MIG, a chemokine that has been shown to chemoattract activated T cells (for a review, see reference 27), might be involved in monocyte recruitment to inflamed lymph nodes. Indeed, the subset of HEVs that express MIG had a dramatically enriched capacity for binding monocytes compared with MIG$^-$ HEVs. In vivo and ex vivo assays showed that inflammation in TNF null mice failed to elicit expression of MIG by HEVs and failed to elicit increased monocyte recruitment via HEVs further strengthening the correlation of MIG expression and monocyte recruitment. More important was the demonstration that MIG neutralizing antibody was able to block inflammation-induced monocyte binding and recruitment both in vitro and in vivo, respectively. Together these data suggest that MIG plays a key role in binding and recruitment of monocytes to HEVs in lymph nodes draining a local inflammatory site.

The differential MIG expression patterns in wild-type and TNF null mice revealed an interesting differential requirement of TNF expression for MIG expression by monocytes and HEVs. Recent studies suggest that TNF expression is upstream of chemokine expression. For example, Czermack et al. (20) showed that TNF neutralizing antibodies reduced chemokine expression in a lung injury model. In another study, TNF null mice had a decreased expression of several chemokines, in particular BLC, in the spleen (21). The downstream effect of the downregulation of chemokine expression in these mice was the loss of primary B cell follicular structure in the spleen, as well

as in the lymph nodes (23, 28). At the message level, MIG is expressed and upregulated upon inflammation in TNF null mice; however, immunostaining revealed that whereas wild-type mice had an increase of MIG^+ HEVs of approximately sixfold with inflammation, inflamed TNF null mice exhibited no such increase (data not shown) and also revealed that MIG is predominantly expressed in macrophage-rich areas within the lymph node. This suggests that low-level, basal expression of MIG is TNF independent; however, the upregulation of MIG on HEVs is TNF dependent.

Previous studies on MIG failed to show chemotaxis of monocytes (29); however, <2% of circulating monocytes express CXCR3, making this population difficult to detect by calcium flux or chemotaxis assays. Selective recruitment of this small population could result in reasonable accumulation of cells to inflammatory sites. Interestingly, the percentage of $CXCR3^+$ monocytes is increased in peripheral blood and synovial fluid monocytes in patients with rheumatoid arthritis (25) compared with normal controls. Indeed, one study has shown the existence of a $CXCR3^+$ population of "plasmacytoid monocytes" that are found in and around inflamed lymph node HEVs (26). Here we also showed that a high percentage of elicited peritoneal monocyte/macrophages also express CXCR3. While the percentage of $CXCR3^+$ peripheral blood monocytes is small, the frequency is increased in chronic inflammation and in populations of recruited monocytes suggesting that selective expression of MIG by endothelium in inflammatory sites could contribute to recruitment of a population of monocytes expressing CXCR3.

Many recent studies have contributed to the strength of the paradigm in which functionally distinct subsets of circulating lymphocytes express unique sets of adhesion molecules and chemokine receptors that allow them access to selected tissues by virtue of tissue-specific expression of the specific receptor ligands (adhesion molecules and chemokines; for a review, see reference 30). The elegant studies of Warnock et al. (18) revealed that the signaling molecules required to recruit lymphocyte subsets are differentially presented by HEVs in functionally distinct microdomains within secondary lymphoid organs, suggesting that functionally distinct microenvironments within a lymph node can selectively recruit leukocyte subsets. We have provided correlative and direct evidence that the lymph node microenvironment can direct the nature of molecules expressed on HEV subsets in a TNF-dependent fashion, that a subset of predominantly perifollicular HEVs in lymph nodes draining an inflammatory site express the CXC chemokine MIG and that this subset of HEVs preferentially support the monocyte-selective increase in adhesion induced by inflammation. Future studies will determine whether other sites of inflammation, particularly chronic inflammation, utilize MIG in the recruitment of monocyte subpopulations.

The authors wish to thank Maribel Andonian and Gary Burget for graphics assistance. The authors especially thank Sirid-Aimee Kellermann, Sigrid Ruuls, Craig Murphy, and Robert Hoek for excellent scientific discussion.

DYNAX Research Institute is supported by Schering-Plough Corporation. This work was funded in part by NIH-R01HL57492-01A1 awarded to L.M. McEvoy.

Submitted: 14 May 2001
Revised: 7 August 2001
Accepted: 6 September 2001

References

1. Sallusto, F., and A. Lanzavecchia. 1994. Efficient presentation of soluble antigen by cultured human dendritic cells is maintained by granulocyte/macrophage colony-stimulating factor plus interleukin 4 and downregulated by tumor necrosis factor α. *J. Exp. Med.* 179:1109–1118.
2. Randolph, G.J., K. Inaba, D.F. Robbiani, R.M. Steinman, and W.A. Muller. 1999. Differentiation of phagocytic monocytes into lymph node dendritic cells in vivo. *Immunity.* 11: 753–761.
3. Navab, M., S.Y. Hama, T.B. Nguyen, and A.M. Fogelman. 1994. Monocyte adhesion and transmigration in atherosclerosis. *Coron. Artery Dis.* 5:198–204.
4. Schmitz, G., A.S. Herr, and G. Rothe. 1998. T-lymphocytes and monocytes in atherogenesis. *Herz.* 23:168–177.
5. Reape, T.J., and P.H. Groot. 1999. Chemokines and atherosclerosis. *Atherosclerosis.* 147:213–225.
6. Uguccioni, M., M. D'Apuzzo, M. Loetscher, B. Dewald, and M. Baggiolini. 1995. Actions of the chemotactic cytokines MCP-1, MCP-2, MCP-3, RANTES, MIP-1α and MIP-1β on human monocytes. *Eur. J. Immunol.* 25:64–68.
7. Kowala, M.C., R. Recce, S. Beyer, C. Gu, and M. Valentine. 2000. Characterization of atherosclerosis in LDL receptor knockout mice: macrophage accumulation correlates with rapid and sustained expression of aortic MCP-1/JE. *Atherosclerosis.* 149:323–330.
8. Rayner, K., S. Van Eersel, P.H. Groot, and T.J. Reape. 2000. Localization of mRNA for JE/MCP-1 and its receptor CCR2 in atherosclerotic lesions of the ApoE knockout mouse. *J. Vasc. Res.* 37:93–102.
9. Gu, L., Y. Okada, S.K. Clinton, C. Gerard, G.K. Sukhova, P. Libby, and B.J. Rollins. 1998. Absence of monocyte chemoattractant protein-1 reduces atherosclerosis in low density lipoprotein receptor-deficient mice. *Mol. Cell.* 2:275–281.
10. Dawson, T.C., W.A. Kuziel, T.A. Osahar, and N. Maeda. 1999. Absence of CC chemokine receptor-2 reduces atherosclerosis in apolipoprotein E-deficient mice. *Atherosclerosis.* 143:205–211.
11. Fife, B.T., G.B. Huffnagle, W.A. Kuziel, and W.J. Karpus. 2000. CC chemokine receptor 2 is critical for induction of experimental autoimmune encephalomyelitis. *J. Exp. Med.* 192:899–905.
12. Izikson, L., R.S. Klein, I.F. Charo, H.L. Weiner, and A.D. Luster. 2000. Resistance to experimental autoimmune encephalomyelitis in mice lacking the CC chemokine receptor (CCR)2. *J. Exp. Med.* 192:1075–1080.
13. Huang, D.R., J. Wang, P. Kivisakk, B.J. Rollins, and R.M. Ransohoff. 2001. Absence of monocyte chemoattractant protein 1 in mice leads to decreased local macrophage recruitment and antigen-specific T helper cell type 1 immune response in experimental autoimmune encephalomyelitis. *J. Exp. Med.* 193:713–726.

14. Picker, L.J., and E.C. Butcher. 1992. Physiological and molecular mechanisms of lymphocyte homing. *Annu. Rev. Immunol.* 10:561–591.
15. Butcher, E.C., and L.J. Picker. 1996. Lymphocyte homing and homeostasis. *Science.* 272:60–66.
16. Bargatze, R.F., M.A. Jutila, and E.C. Butcher. 1995. Distinct roles of L-selectin and integrins α4β7 and LFA-1 in lymphocyte homing to Peyer's patch-HEV in situ: the multistep model confirmed and refined. *Immunity.* 3:99–108.
17. von Andrian, U.H., and C.R. Mackay. 2000. T-cell function and migration. Two sides of the same coin. *N. Engl. J. Med.* 343:1020–1034.
18. Warnock, R.A., J.J. Campbell, M.E. Dorf, A. Matsuzawa, L.M. McEvoy, and E.C. Butcher. 2000. The role of chemokines in the microenvironmental control of T versus B cell arrest in Peyer's patch high endothelial venules. *J. Exp. Med.* 191:77–88.
19. McEvoy, L.M., M.A. Jutila, P.S. Tsao, J.P. Cooke, and E.C. Butcher. 1997. Anti-CD43 inhibits monocyte-endothelial adhesion in inflammation and atherogenesis. *Blood.* 90:3587–3594.
20. Czermak, B.J., V. Sarma, N.M. Bless, H. Schmal, H.P. Friedl, and P.A. Ward. 1999. In vitro and in vivo dependency of chemokine generation on C5a and TNF-α. *J. Immunol.* 162:2321–2325.
21. Ngo, V.N., H. Korner, M.D. Gunn, K.N. Schmidt, D.S. Riminton, M.D. Cooper, J.L. Browning, J.D. Sedgwick, and J.G. Cyster. 1999. Lymphotoxin α/β and tumor necrosis factor are required for stromal cell expression of homing chemokines in B and T cell areas of the spleen. *J. Exp. Med.* 189:403–412.
22. Pryhuber, G.S., D.P. O'Brien, R. Baggs, R. Phipps, H. Huyck, I. Sanz, and M.H. Nahm. 2000. Ablation of tumor necrosis factor receptor type I (p55) alters oxygen-induced lung injury. *Am. J. Physiol. Lung Cell. Mol. Physiol.* 278: L1082–L1090.
23. Korner, H., M. Cook, D.S. Riminton, F.A. Lemckert, R.M. Hoek, B. Ledermann, F. Kontgen, B. Fazekas de St Groth, and J.D. Sedgwick. 1997. Distinct roles for lymphotoxin-α and tumor necrosis factor in organogenesis and spatial organization of lymphoid tissue. *Eur. J. Immunol.* 27:2600–2609.
24. Stamper, H.B., Jr., and J.J. Woodruff. 1976. Lymphocyte homing into lymph nodes: in vitro demonstration of the selective affinity of recirculating lymphocytes for high-endothelial venules. *J. Exp. Med.* 144:828–833.
25. Katschke, K.J., Jr., J.B. Rottman, J.H. Ruth, S. Qin, L. Wu, G. LaRosa, P. Ponath, C.C. Park, R.M. Pope, and A.E. Koch. 2001. Differential expression of chemokine receptors on peripheral blood, synovial fluid, and synovial tissue monocytes/macrophages in rheumatoid arthritis. *Arthritis Rheum.* 44:1022–1032.
26. Cella, M., D. Jarrossay, F. Facchetti, O. Alebardi, H. Nakajima, A. Lanzavecchia, and M. Colonna. 1999. Plasmacytoid monocytes migrate to inflamed lymph nodes and produce large amounts of type I interferon. *Nat. Med.* 5:919–923.
27. Farber, J.M. 1997. Mig and IP-10: CXC chemokines that target lymphocytes. *J. Leukoc. Biol.* 61:246–257.
28. Pasparakis, M., L. Alexopoulou, V. Episkopou, and G. Kollias. 1996. Immune and inflammatory responses in TNF α-deficient mice: a critical requirement for TNF α in the formation of primary B cell follicles, follicular dendritic cell networks and germinal centers, and in the maturation of the humoral immune response. *J. Exp. Med.* 184:1397–1411.
29. Liao, F., R.L. Rabin, J.R. Yannelli, L.G. Koniaris, P. Vanguri, and J.M. Farber. 1995. Human MIG chemokine: biochemical and functional characterization. *J. Exp. Med.* 182: 1301–1314.
30. Campbell, J.J., and E.C. Butcher. 2000. Chemokines in tissue-specific and microenvironment-specific lymphocyte homing. *Curr. Opin. Immunol.* 12:336–341.